PHYSICAL REVIEW B VOLUME 17, NUMBER 4 15 FEBRUARY 1978

Many-valley interactions in n-type silicon inversion layers

G. Dorda, I. Eisele, and H. Gesch
Forschungslaboratorien der Siemens AG, München, Germany
(Received 4 April 1977)

Correlation effects between different conduction-band valleys have been studied experimentally for electrons in silicon inversion layers. The quantized subband systems were energetically shifted relative to each other by a uniaxial mechanical stress which modifies the conditions favoring intervalley coupling. Transport investigations such as magnetoquantum oscillations, piezoresistance, Hall mobility, and anisotropic conductivity were analyzed with respect to effective masses and relaxation times for (100), (110), and (111) surface orientations. All results are consistent with a domain model on the basis of charge-density waves as a stable ground state. A domain size of the order of 250 nm has been estimated for the (111) surface. The relaxation time has been found to be anisotropic for elliptical subbands.

I. INTRODUCTION

In recent years great attention has been devoted to the quasi-two-dimensional electron gas in inversion and accumulation layers of semiconductor-insulator interfaces. Along with the rapid development of metal-insulator-semiconductor (MIS) technology physical properties at the semiconductor surface such as surface states, transport of charge carriers, and optical properties have been investigated. The main feature of a MIS sandwich structure is a band bending near the semiconductor surface which can be achieved by applying an electric field between the metal and the semiconductor. Depending on the sign of the field, an accumulation or depletion of the majority-carrier density occurs. Of special interest is the inversion layer, where the band bending is so large that the minority-carrier density exceeds the majority-carrier bulk density. The capacitively induced charge carriers in the inversion layer are confined within an approximately 10-nm-wide one-dimensional potential well normal to the interface. The considered layer is limited by the semiconductor surface and the depletion layer which acts like a p-n junction and isolates the induced mobile carriers from the bulk. The energy of charge carriers in such a potential well is quantized.[1]

Progress during the past few years has enlightened the understanding of the p-type inversion layer considerably, whereas at the same time unsolved problems seemed to pile up for n-type layers. Several authors[2-4] report an anomalous valley degeneracy of 2 for the ground state of the (110) and (111) surface instead of the theoretically predicted fourfold and sixfold degeneracy, respectively. It is also surprising that the effective mass has a pronounced dependence on mechanical stress[5,6] and temperature.[7] Furthermore, it is puzzling that the conductivity for the (111) surface is isotropic,[4,8] despite the measured valley degeneracy of 2. A theoretical attempt to overcome these apparent discrepancies has been made by Kelly and Falicov,[9,10] who calculated the interactions of electrons in subbands of different valleys. The present paper provides several supplementary experiments which are analyzed with respect to this theory. For this purpose we measured piezoresistance, anisotropic conductivity, and Shubnikov–de Haas (SdH) oscillations under tensile and compressive mechanical stress for (100), (110), and (111) n-type Si inversion layers.

II. THEORETICAL ASPECTS

The experimental methods used within the framework of this paper are mainly related to the mobility, i.e., the transport masses and the relaxation times of electrons in the n-type inversion layer. Because the effective masses and the relaxation time τ depend strongly on mechanical stress, the existing discrepancies seem to be related to correlation effects between electrons in different subbands. Depending on electron concentration and temperature, τ is determined by phonon scattering, surface roughness, and ionic impurities. The effect of acoustic and optical phonons on mobility has been studied extensively[11-13] for the intravalley case and recently intersubband intravalley scattering has been added.[14] The first and only approach to include intervalley electron-phonon interactions for a two-dimensional electron gas was made for the (111) surface.[9] The calculations for the ground state of the inversion layer yield stable solutions for the ordinary paramagnetic state, the ferromagnetic occupation of one valley, and finally for charge-density waves (CDW) and spin-density waves (SDW), respectively. For silicon SDW can be omitted and essentially only the paramagnetic and the CDW

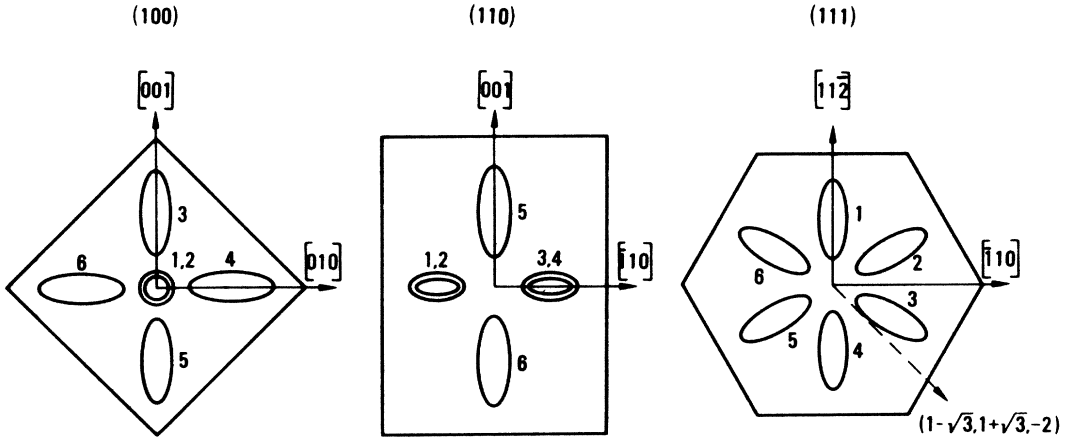

FIG. 1. Constant-energy ellipses and Brillouin zones of the two-dimensional electron gas in silicon inversion layers on (100), (110), and (111) surfaces.

states are probable. Independent of surface orientation, the latter results in a degeneracy of 2, whereas the degeneracy of the paramagnetic state depends on surface orientation, yielding 2 for the (100) surface, 4 for (110), and 6 for (111).[15] For the band structure of Si surfaces (see Fig. 1) the simplest case for the intervalley exchange correlation is the (111) surface, where the ground states of the six valleys are equal and independent of the electric surface field. For the (110) surface only the four energetically lowest ground states (1,...,4 in Fig. 1) must be taken into account for intervalley exchange. The two remaining valleys can be disregarded for the quantum-limit case. Finally, for the (100) surface two ground states (1, 2 in Fig. 1) are normally populated. Thus only the paramagnetic state is possible under normal conditions. If the discussed model is correct the intervalley exchange interaction can lead to CDW's whenever two subbands of right-angle valleys approach each other. From this point of view it is an interesting idea to shift the conduction-band valleys relative to each other which can be done by applying uniaxial mechanical stress.[16] The result should be creation or annihilation of correlation effects.

A. Piezoresistance

Under mechanical stress P the energy difference $\partial E_j - \partial E_i$ between two valleys changes according to[17]

$$\partial E_j - \partial E_i = (S_{11} - S_{12})\Xi_u(P_i - P_j)\,, \tag{1}$$

where i and j are the components along the main crystallographic axes. S_{11} and S_{12} are the elastic compliance coefficients, and Ξ_u is the deformation-potential constant. The change of the relative energy position can cause an electron transfer between different valleys. If the mobilities in these valleys are not identical one obtains a longitudinal-resistance change $\Delta\rho_x(P)/\rho_x(P=0)$ which depends on effective mass m and relaxation time τ,

$$\frac{\Delta\rho_x(P)}{\rho_x(P=0)} = \frac{\left(\frac{\tau_{xm}}{m_{xm}} - \frac{\tau_{xl}}{m_{xl}}\right)\Delta n_{lm}}{n_m\frac{\tau_{xm}}{m_{xm}} + n_l\frac{\tau_{xl}}{m_{xl}}}\,, \tag{2}$$

where the index x labels an arbitrary current direction and l, m are the indices of two different valleys. The concentration of a two-dimensional electron gas is given by Fermi-Dirac statistics,

$$n = \frac{kT}{\pi\hbar^2}(m_1 m_2)^{1/2}\ln\left[1 + \exp\left(\frac{E_F - E_0}{kT}\right)\right]. \tag{3}$$

Here a factor of 2 for spin has been included. m_1 and m_2 are the principal effective masses for motion parallel to the surface, E_F is the Fermi level, and E_0 the ground state of a single subband. The population of more than one subband can be resolved with Eq. (3) and the law of charge conservation,

$$\sum_l \Delta n_l = 0\,. \tag{4}$$

Considering only the ground states E_0 of different valleys, one obtains at low temperatures ($E_F - E_0 \gg kT$) with the proper valley degeneracy g_v

$$\Delta n_{lm} = \frac{1}{\pi\hbar^2}\frac{(m_{xm}m_{xl})^{1/2}}{(m_{xm})^{1/2} + (m_{xl})^{1/2}}(\partial E_{0l} - \partial E_{0m})$$

$$= \frac{1}{\pi\hbar^2}\frac{(m_{xm}m_{xl})^{1/2}}{(m_{xm})^{1/2} + (m_{xl})^{1/2}}(S_{11} - S_{12})\Xi_u(P_i - P_j)\,, \tag{5}$$

where P_i and P_j are the mechanical stress components along the main crystallographic axis of valleys m and l, respectively. Equations (2) and (5) deliver a general description of the piezoresistance at low temperatures.

B. Anisotropic Conductivity

The anisotropic conductivity proves to be an excellent tool to check the charge carrier distribution between isotropic and anisotropic subbands. The method has been used earlier for (110) n-type inversion layers.[18] This section describes the results if an energy shift due to mechanical stress is included. An electric field E with an arbitrary direction x in the surface plane causes a current flow according to

$$\sum_l g_{xl} = \sum_l \frac{e^2 n_l \langle \tau_{xl} \rangle}{m_{xl}} E_x . \tag{6}$$

If the subband is anisotropic and E_x is not in the direction of a principal axis, a perpendicular component E_y of the electric field appears which can be evaluated with the following equilibrium condition:

$$\sigma_{yx} E_x + \sigma_{yy} E_y = 0 . \tag{7}$$

Supposing an isotropic relaxation time τ and introducing the angle α between the applied electric field direction x and the large semiaxis of the considered anisotropic subbands, we obtain

$$\frac{E_y}{E_x} = \frac{\sum_l n_l \sin\alpha_l \cos\alpha_l (m_{2l} - m_{1l})}{\sum_l n_l (m_{2l} \cos^2\alpha_l + m_{1l} \sin^2\alpha_l)} . \tag{8}$$

The indices 1 and 2 correspond to the effective masses along the principal axis of the two-dimensional subband ($m_1 < m_2$).

C. Magnetic Quantum Oscillations

In general, high magnetic fields quantize the conduction band into Landau levels.[19] This causes an oscillatory magnetoresistivity (Shubnikov–de Haas oscillations) with a periodicity given by[20]

$$\frac{\Delta\rho}{\rho} = A \cos\left[\frac{2\pi(E_F - E_0)m_c}{\hbar e B} - \Delta\rho\right] , \tag{9}$$

where A is the amplitude, E_0 the lowest energy level of the conduction band, m_c the effective mass, and B the magnetic field. It should be noted that Eq. (9) is restricted to a model which assumes isotropic and elastic scattering. In this case $\Delta\varphi$ depends on the density of states and becomes $\pi/4$ for the three-dimensional case and zero for two dimensions.[21] Despite the fact that $\Delta\varphi$ is influenced by the assumed scattering model it does not enter significantly our analysis because experimentally no phase changes could be detected. Considering that the two-dimensional density of states is independent of energy[1] the following modification of Eq. (9) can be obtained for identical degenerate subbands:

$$\frac{\Delta\rho}{\rho} = A \cos\left(\frac{2\pi h}{e g_s g_v} \frac{n}{B}\right), \tag{10}$$

where n is the electron concentration and g_s and g_v are the spin and valley degeneracy factors, respectively. It should be noted that for the two-dimensional case the periodicity is independent of the effective mass. The amplitude of the magnetoresistance can be rewritten in the following form:

$$A = 5kTm_c \left(\frac{2g_s g_v}{h^3 enB}\right)^{1/2} \frac{\exp(-am_c T_D/B)}{\sinh(am_c T/B)} , \tag{11}$$

$$a = 2\pi^2 k/\hbar e ,$$

where the Dingle temperature T_D characterizes the collision broadening of the oscillations. It can be evaluated from the ratio of the amplitudes at different magnetic fields. In the region where T_D is independent of temperature, the effective mass can be calculated from the temperature dependence of the SdH amplitudes. To obtain accurate mass values several restrictions are required. The fitting procedure of the amplitudes can be applied if the oscillations are sinusoidal, i.e., spin and valley splitting can be neglected. Moreover, Ando[22] points out that the equation for the amplitudes is only valid for rather weak magnetic fields ($\omega_c \tau \lesssim 1$, where ω_c is the cyclotron frequency and τ the relaxation time for the charge carriers). For our analysis both limits were verified by selecting oscillations for magnetic fields which yield $\omega_c \tau \leq 2$. In order to avoid contributions from higher harmonics it is furthermore necessary that $kT > eB\hbar/2\pi^2 m_c$.[20] For the reported experiments the thermal energy varied between $0.14 < kT < 0.3$ meV which for an effective mass $m_c = 0.2 m_0$ limits the magnetic field B to approximately 5 T. In addition, the temperature interval for the determination of the effective cyclotron mass has to be chosen carefully because at too low a temperature the SdH amplitudes saturate when the half-widths of the Landau levels are no longer a function of temperature.

If the electron concentration is determined either capacitively or from Hall measurements, the valley degeneracy g_v can be deduced from the periodicity of SdH oscillations. Furthermore, if by applying mechanical stress more than one type of subband is populated, the analysis of SdH yields information about the electron distribution between these subband systems. One disadvantage

of the SdH method as compared to piezoresistance and anisotropic conductivity is its limitation to low temperatures (<10 K) in order to realize the oscillatory character of the magnetoresistance.

III. EXPERIMENTAL

The devices were Hall bars with a length of 400 μm and a width of 40 μm. By using a four-probe geometry the influence of contact problems at source and drain was avoided and the accurate determination of the electron conductivity was guaranteed. n-channel metal-oxide-semiconductor (MOS) transistors on (100), (110), and (111) 4–7-cm p-type silicon wafers were fabricated. The oxide had a thickness of 120 nm and was thermally grown at 1050 °C. The aluminum gate was deposited at 80 °C and had a thickness of 1 μm. Besides these mostly used devices, samples with a different oxide thickness of 60 nm and silicon as gate material were checked for comparison. Except for the interface quality which influences the mobility, no differences have been observed. Based on mobility profile calculations[23] we can state that for our silicon-gate samples the amount of potential fluctuations is smaller. The isotropic pre-existing interface stress originating from a sandwich structure of Si-SiO_2-Al has also been determined for the temperature range between 4.2 and 300 K. It does not exceed 10 N/mm^2 and is small compared to the externally applied uniaxial mechanical stress.[24]

Narrow slabs 0.8×16 mm^2 with one row of transistors were cut from wafers containing transistor arrays. The slab was mounted on one end, whereas the free end was bent upwards or downwards. The resulting stress is uniaxial and its inhomogeneity across the depth of the space-charge layer is negligible because the channel thickness of the MOS field-effect transistor (MOSFET) is less than 100 nm compared to 0.25 mm of the sample slab. The resulting surface stress P can be calculated according to usual mechanics,[16]

$$P = 6(l/wt^2)Q\,, \tag{12}$$

where l is the length between the load Q and the transistor and w and t are width and thickness of the slab, respectively. The maximum achieved stress of ~350 N/mm^2 was limited by the breaking point of the slab. With this value and the deformation potential constant of the bulk ($\Xi_u = 8.6$ eV) Eq. (1) yields a maximum energy shift $\Delta E = 31$ meV of two valleys relative to each other.

The cryostat containing the stress arrangement with the mounted sample was located in a superconducting magnet. The mechanical stress was applied after achieving the desired temperature and was normally released whenever the temperature was varied. Several temperature and stress cycles over the whole measuring range yielded reproducible data. Temperature variations between 1.3 and 400 K have been used. The Hall mobility has been determined at a magnetic field of 1 T and for the SdH oscillations the magnetic field was swept between 0 and 9 T with a constant electron concentration, i.e., gate field. All measurements were restricted to drift fields below 0.1 V/cm in order to exclude any warm-electron effects.

The reproducibility of the results was not only tested with respect to temperature and stress, but also in relation to device fabrication. For all three surface orientations several transistors from four wafers of two different batches have been selected and for each surface orientation the results agreed quite well.

IV. RESULTS AND DISCUSSION

A. Effective Masses under Stress

Effective masses have been determined with and without uniaxial stress (tension as well as compression) for (100), (110), and (111) surface orientations. For the evaluation of the SdH amplitudes it is necessary to check carefully the Dingle temperature T_D because a temperature-dependent T_D leads to wrong mass values. An iterative calculation of T_D and m_c has been carried out by evaluating the amplitude sequence at a given temperature as well as the temperature dependence of the amplitudes for a constant magnetic field. It turned out that T_D is not always temperature independent. Therefore, the following data were obtained from selected samples where the temperature dependence of T_D introduced an error which was far below the measurement accuracy of 15%. The oscillatory magnetoresistance was measured by means of potential probes in order to avoid contact effects. Simultaneously to an analog recording, the signal was digitized and twice differentiated. This enables one to determine very accurately the sinusoidal shape, i.e., the absence of the harmonic content of the oscillations. Furthermore, this procedure yields the precise magnetic field for the extrema. For electron concentrations below 2×10^{12} cm^{-2} due to the harmonic content the evaluation of the amplitudes was restricted to magnetic fields up to 4 T, whereas at higher concentrations the mass extraction was possible up to 6 T. For better accuracy the SdH oscillations were measured at three temperatures, namely, 1.7, 2.5, and 3.5 K. Thus the error of the shown mass data was kept below 15%. Under

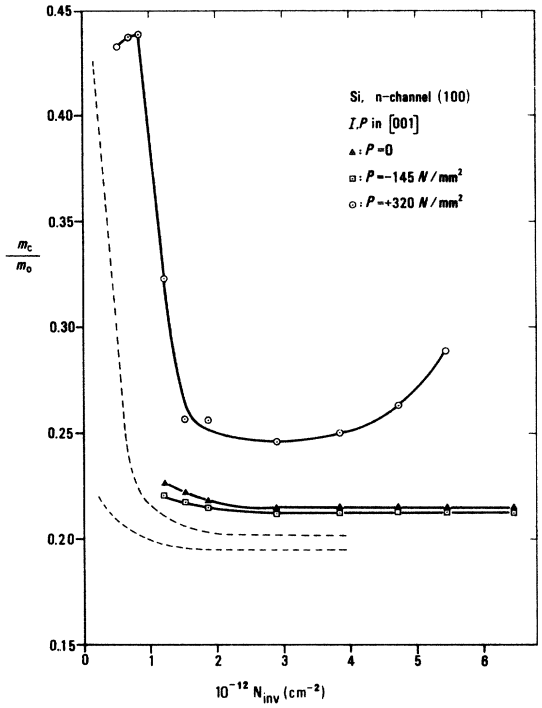

FIG. 2. Stress-dependent effective mass m_c/m_0 plotted against electron concentration N_{inv} in the inversion layer for a (100) surface. Current I and stress P in [001] direction. ▲, without stress; ⊙, compression; □, tension. For comparison the dashed lines represent cyclotron resonance data for $P=0$ (lower profile) and compression $P=150$ N/mm^2 (upper profile).

tension as well as compression no change of the line shape has been found.

Our goal was to deduce intersubband electron-transfer effects and the corresponding valley degeneracy g_v. For a given gate field, i.e., constant electron concentration, $E_F - E_0$ for one particular subband depends on the distribution of electrons among all subbands. According to Eq. (9) any deviation of $E_F - E_0$ is followed by a periodicity change of the SdH oscillations. Application of stress is expected to cause electron-transfer effects which lead to a change in $E_F - E_0$ [see Eq. (10)]. It is evident that more than one set of oscillations appears whenever $(E_F - E_0)m_c$ differs for different subbands. Moreover, if the concentration effect Δn originates from a transfer into unpopulated subbands and not from trapping into surface states[25] we expect the appearance of a new oscillation. The experiments contradict these expectations: for all orientations the periodicity is completely stress independent (typical SdH oscillations with and without stress have been presented in an earlier paper[5]), whereas the effective mass changes in Figs. 2–4 are considerable. (The effective-mass changes due to the stress-induced deformation of the silicon lattice should be $\Delta m_c/m_c \leq 1.5\%$ for a stress $P=320$ N/mm^2.[26]) For this case Eq. (11) predicts amplitude modifications but the measured and the calculated values disagree by far. Furthermore, the ground-state degeneracy remains 2, independent of stress, electron concentration, and surface orientation.[4,27] Sec. IV B analyzes the anomalies of the SdH data for all three surface orientations and shows that a full description is only possible if intervalley correlations are assumed.

For the (100) surface Fig. 2 exhibits the effective-mass changes under tension ($P<0$) and compression ($P>0$) versus concentration of mobile electrons N_{inv}. Of interest are the pronounced asymmetry of the stress influence and the large-mass change due to compression. In the unstressed quantum-limit case only valleys 1 and 2 are populated (Fig. 1) and the SdH analysis yields the well-known mass data.[28] Valleys 3–6 are in general unpopulated[29] and intervalley interactions with these valleys can be disregarded. Compression in [001] direction lessens the energy separation $\Delta E = E_0' - E_0$ between the ground states of valleys 3–5 and 1–2, respectively. For $P=320$ N/mm^2 the stress-induced energy shift becomes 27 meV and in comparison with theoretical calculations[30] both energy levels are equal for an electron concentration of approximately 1.5×10^{12} cm^{-2}. At lower concentrations a crossing occurs and eventually only valleys 3 and 5 are populated ($N_{inv}<5\times10^{11}$ cm^{-2}). At higher concentrations the splitting due to quantization exceeds the energy shift due to compression and the electron transfer into valleys 3–5 decreases. It should be noted that in general the Fermi level $E_F - E_0$ increases faster than $E_0' - E_0$. As a consequence the electron transfer increases again beyond a certain surface field.

In connection with the described population effect, intervalley interaction can take place. The necessity of introducing correlation effects can be deduced from the experimental fact that the valley degeneracy remains 2 even if valleys 1–2 and 3–5 are populated under stress. According to theory[9,10] the description of the intervalley coupling leading to CDW's holds whenever electrons occupy more than two valleys. In this case two particular valleys are populated, whereas the others are energetically raised, which leads to $g_v=2$. Valleys 1–2 and 3–5 obey this condition and CDW states are favored around $N_{inv}=1.5\times10^{12}$ cm^{-2} and above 5×10^{12} cm^{-2}. The effective masses of electrons in coupled valleys should be in between the value for the isotropic subbands 1–2 with $m_c = 0.21m_0$ and the anisotropic subbands 3–5 with

$m_c = 0.43 m_0$. At least four equivalent combinations of right-angle valleys are possible which causes the existence of a domain structure in the inversion layer.[27] If CDW regions and the paramagnetic state exist simultaneously, but in different regions, the observed m_c should be lower. This behavior has indeed been seen, as is shown in Fig. 2. The saturation value below $N_{inv} = 8 \times 10^{11}$ cm^{-2} is related to the cyclotron mass of the anisotropic subbands. It hints that valleys 1–2 are lifted way above 3–5 and thus the intersubband correlation is almost nonexistent.

For tension in [001] direction the energy separation between valleys 1–2 and 3–5 is increased, whereas valleys 4–6 remain unchanged with respect to 1–2. Evidently no significant population effects occur and only diminishing mass changes due to lattice distortion are expected, which is in excellent agreement with the experimental data.

For comparison, cyclotron resonance mass data[6] are shown in Fig. 2. The unstressed mass values are in the whole concentration range about 10% lower. This is the usual difference between the mass determination from cyclotron resonance and SdH measurements and could be due to the different electron motion: for SdH in addition to the magnetic-field-induced circular-electron motion an electric-drift field moves the electrons along the channel. Under compression the profile with a maximum $m_c = 0.42 m_0$ agrees qualitatively with our measurements. The deviation results from the lower applied stress value of 150 N/mm^2.

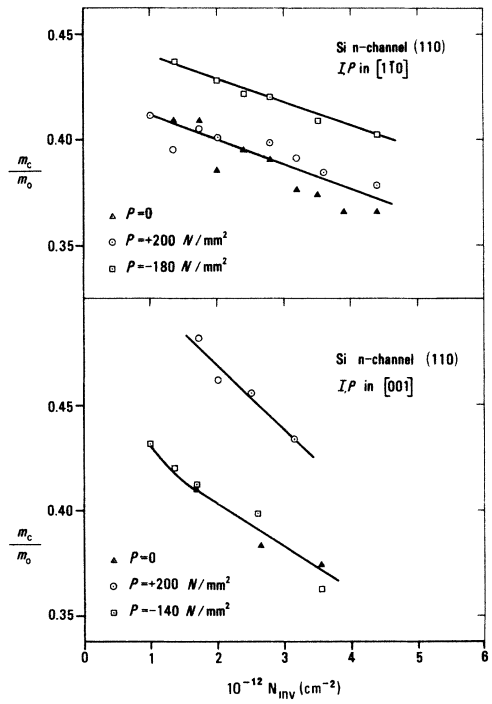

FIG. 3. Stress-dependent effective mass m_c/m_0 as a function of electron concentration N_{inv} for a (110) surface. The data are plotted for current I and stress P in [1$\bar{1}$0] and [001] direction, respectively. ▲, without stress; ⊙, compression; □, tension.

A similar analysis has been carried out for the (110) surface orientation with uniaxial stress in [1$\bar{1}$0] and [001] direction, respectively. Two different stress directions have been chosen in order to disprove the argument that a pre-existing uniaxial stress lifts the valley degeneracy. One crucial experimental result is the unavoidable valley degeneracy $g_v = 2$ which is independent of any electron-transfer effects caused by mechanical stress. The unstressed mass values in Fig. 3 agree quite well with other published data.[2] Of importance is a mass increase for compression in [001] direction as well as tension in [1$\bar{1}$0] direction. No Δm_c effect occurs for reversing the sign of the stress in these directions. The unstressed ground state of the (110) orientation is an equal population of valleys 1–3 and 2–4. From Fig. 1 it can be concluded that tension in [1$\bar{1}$0] direction causes a transfer into 5–6 which finally will be the only populated valleys for low-electron concentrations. A similar behavior sets in for compression in [001] direction with the only difference that the energy shift $\Delta E(P)$ is twice as large because the stress is along the main crystallographic axis. The experimental results in Fig. 3 confirm this consideration. In connection with $g_v = 2$, the large-mass changes due to electron transfer can only be interpreted by intervalley correlation between the subbands 1–3, 2–4, and 5–6 and not by preexisting stress. Domains resulting from the correlation model exist already for the ground state of the unstressed system and their annihilation is possible for compression in [001] direction.

Figure 4 exhibits the effective-mass values for the (111) surface. The uniaxial stress has been chosen in [1$\bar{1}$0] direction (see Fig. 1). The interpretation of the results is again given on the basis of the correlation model. The right-angle valleys 2-3-5-6 remain populated under compression and we suppose that a configuration with domains should always exist. Indeed no mass changes occur. Tension results in the population of valleys 1 and 4 which are situated along a main axis and evidently the paramagnetic state should be approached. This leads to the mass decrease in Fig. 4. The observed masses under tension suggest that CDW coupling increases the cyclotron mass for the (111) surface which has been predicted.[9] The energy shift for $P = -220$ N/mm^2

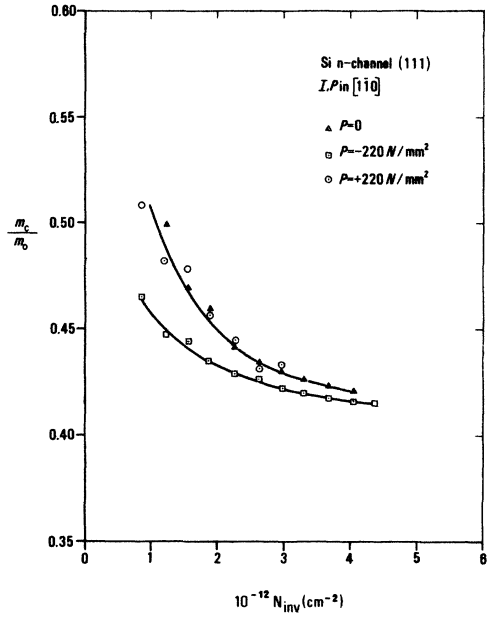

FIG. 4. Stress-dependent effective mass m_c/m_0 plotted against electron concentration N_{inv} for a (111) surface. Current I and stress P in [1$\bar{1}$0] direction. ▲, without stress; ⊙, compression, □, tension.

amounts to $\Delta E = 9.5$ meV and therefore the paramagnetic state has probably not been reached completely.

Besides the effective masses it is worthwhile to mention the influence of mechanical stress on the amplitude height of the SdH oscillations. In a previous publication[5] we showed that for the (100) surface compression causes a tremendous decrease of the amplitudes. For the (110) surface the same amount of compression when applied in [001] direction increases the amplitudes remarkable, whereas no appreciable effect occurs for stress in [110] direction. These phenomena are in excellent agreement with the idea of creation [for the (100) surface] and annihilation {for the (110) surface with P in [001] direction} of domains. It turns out that domain wall scattering is responsible for the damping of the amplitudes.[4] The experiments for the (111) surface agree completely with these considerations. Because the unstressed state favors domains, the amplitudes increase or remain unchanged for the different stress directions.

B. Piezoresistivity and Hall Mobility

For the (100) surface, piezoresistance data with current in [010] and stress in [001] direction are presented in Fig. 5. To prove intervalley interactions we prefer these directions to the earlier presented parallel configuration[27] because in the quantum limit no change of the transport mass in current direction is expected and thus the piezoresistance depends mainly on deviations of the relaxation time. The measured profile (Fig. 5) indicates with increasing compression a steep resistivity increase which is followed by a rapid decrease. For the discussion three relaxation-time effects have to be taken into account: (a) different relaxation times for the isotropic and anisotropic valleys, (b) surface-state scattering, (c) intervalley scattering, and (d) domain-wall scattering. The first possibility can be excluded because the electron transfer between isotropic and anisotropic valleys always has to be a gradual transition between two saturation values without any extrema. Surface-state scattering plays a role whenever the Fermi level crosses the energy level

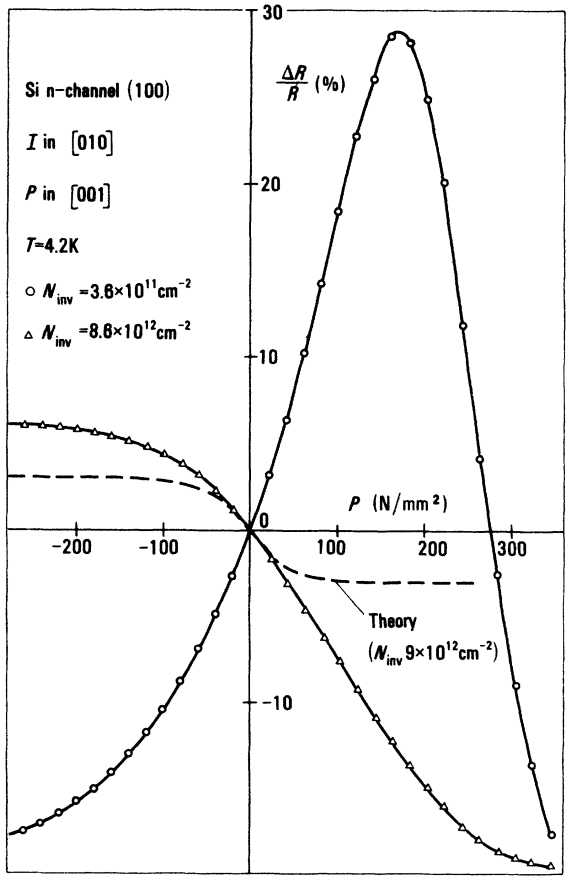

FIG. 5. Stress-induced relative resistance change $\Delta R/R$ at 4.2 K for a (100) surface orientation. Current flow I in [010] and stress P in [001] direction (transverse case). Parameter is the electron concentration N_{inv}. The dashed line represents a theoretical calculation without correlation effects.

of these states. Compression can cause such an effect if the surface states are energetically bound to the anisotropic subband. The maximum interaction according to Fig. 5 appears at $P = 175$ N/mm^2 corresponding to an energy shift $\Delta E(P) = 15$ meV. For $N_{inv} = 3.6 \times 10^{11}$ cm^{-2} the theory[30] for the unstressed condition yields $E_0' - E_0 = 16$ meV. For the considered P and N_{inv}, E_0 and E_0' are therefore energetically nearly equal. From mobility measurements[25] it has been deduced that surface states related to the E_0' subband are at least 6 meV below the subband edge. Thus it seems to be unlikely that surface-state scattering is the origin of the observed resistivity peak. From bulk measurements it is known that intervalley scattering has to be taken into account above 100 K. Despite the fact that the energy of the optical phonons has not been determined at the surface, it seems unlikely that at temperatures as low as 4.2 K this scattering mechanism is of any importance. As has been stated earlier, we believe that the anomalous piezoresistance effect results from intervalley coupling which leads to four different CDW configurations. Despite the fact that they are energetically equal, potential wells should exist at the domain boundaries. This leads to a scattering effect with a maximum at $E_0 \approx E_0'$.

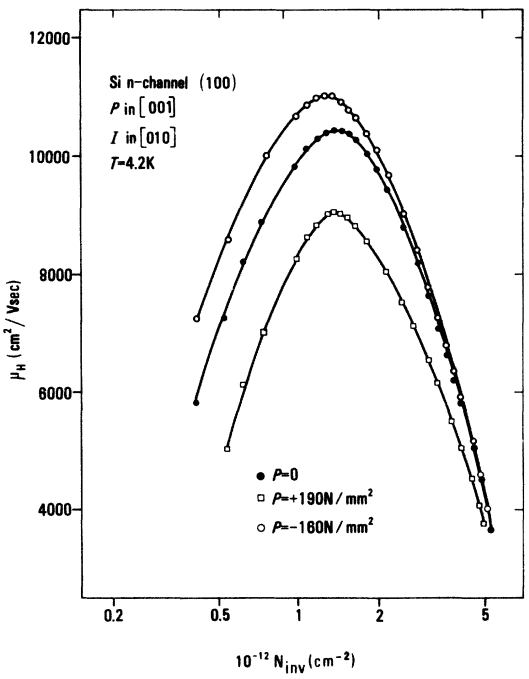

FIG. 6. Stress-dependent Hall mobility μ_H plotted against electron concentration N_{inv} for a (100) surface orientation at 4.2 K (magnetic field $B = 1$ T). Current I in [010] and stress P in [001] direction. •, without stress; □, compression; ○, tension.

At high-electron concentrations the quantum-limit condition is not fulfilled anymore and according to theory approximately 10% of the electrons are distributed among the anisotropic valleys and the first excited subband of the isotropic valleys. With Eq. (5) the piezoresistance effect for $N_{inv} = 9 \times 10^{12}$ cm^{-2} was calculated with help of the "classical" population model and is depicted in Fig. 5. The data for the position of the Fermi level and the quantized energy levels were taken from Stern.[31] Apparently the experimental profile agrees qualitatively but deviates remarkably in magnitude. The discrepancy cannot be fully understood at the moment but the cause might be again a lifting of the intervalley interaction.

With the same transverse configuration as for the piezoresistivity the Hall mobility μ_H is plotted in Fig. 6 versus electron concentration N_{inv}. The characteristic profile with an increase at low concentrations and decrease at high concentrations has already been discussed.[23,32] The electron transfer caused by mechanical stress is accompanied by relaxation-time effects as has been proposed above. In agreement with piezoresistivity, pronounced changes occur at low concentrations, whereas the mobilities almost merge for high concentrations. An explanation of the results with help of stress-induced inhomogeneity changes at the Si-SiO_2 interface seems to be unlikely. At low-electron concentrations a deviation in the transport properties should be related to a change of the ion concentration at the interface. Combined with this effect, a shift of the threshold voltage should occur. This behavior has not been found. Furthermore, inhomogeneities have to be monotonic increasing or decreasing with stress, which contradicts the piezoresistance in Fig. 5. Another indication of the absence of surface states N_{ss} is given by measuring the mobility ratio μ_H/μ_{eff}.[33] Therefore we believe that the mobility behavior is a second experimental verification of the necessity of introducing intervalley coupling for the description of the (100) surface.

To confirm the (100) data we also measured the piezoresistivity for the (110) surface with current in $[1\bar{1}1]$ and mechanical stress in [001] direction. Once more this special configuration depicts only relaxation-time effects and is comparable to the just-described (100) problem. The experimental results are very similar and can be explained with the same ideas. Hall mobility data were reported earlier[5] and are in full agreement with the correlation model including mass and domain effects.

For the (111) surface the stress was applied in the $(1-\sqrt{3}, 1+\sqrt{3}, -2)$ direction (see Fig. 1). The sixfold degeneracy is then reduced into three pairs

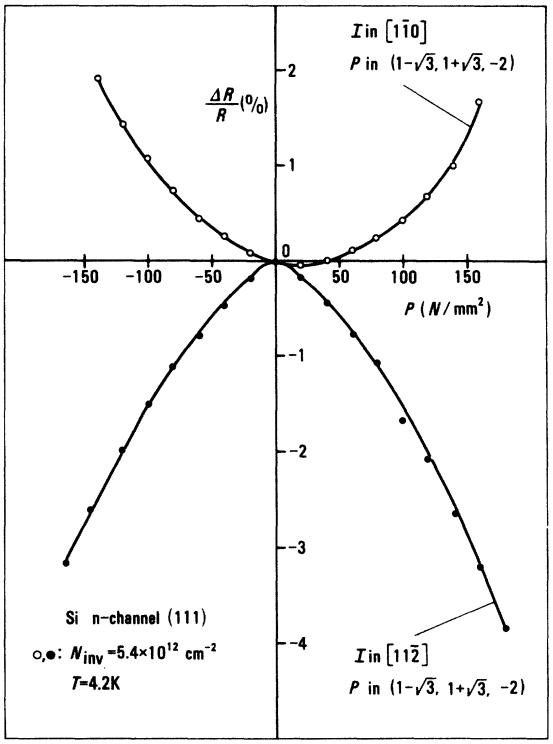

FIG. 7. Stress-induced relative resistance change $\Delta R/R$ at 4.2 K for a (111) surface orientation. Stress P in $(1-\sqrt{3}, 1+\sqrt{3}, -2)$ direction and current I in $[1\bar{1}0]$ and $[11\bar{2}]$ direction, respectively.

of ellipses with equal energy separation ΔE,

$$\Delta(E_3 - E_1) = \Delta(E_1 - E_5) = \tfrac{1}{2}\Delta(E_3 - E_5) = (\sqrt{3}/6)(S_{11} - S_{12})\Xi_u P, \quad (13)$$

where P is the total stress in the given direction. This configuration causes an electron transfer between valleys 3 and 5 as well as 6 and 2 (the concentrations in valleys 1 and 4 remain unchanged). Consequently, no resistivity effect is expected because neither mass changes nor relaxation-time effects occur for current in the $[11\bar{2}]$ and $[\bar{1}10]$ directions. However, there is a parabolic and mirrorlike piezoresistivity effect for the two current directions (see Fig. 7).

The earlier proposed domain model by Tsui and Kaminsky[8] which is based on large inhomogeneous stresses at the Si-SiO_2 interface cannot explain the data in Fig. 7 if it is taken into account that the valley degeneracy never exceeds $g_v = 2$. Moreover the inhomogeneous stresses necessary for this model have to be above 1000 N/mm², whereas recent measurements at low temperatures showed that pre-existing stresses in the inversion layer do not exceed 10 N/mm².[24] In contrast domains initiated by CDW describe the results as satisfactory: according to Eq. (13) stress leads to an energy separation of the valleys which weakens intervalley correlations. This implies the annihilation of domains with a preferable population of valleys 3 and 6 (compression) or 5 and 2 (tension). Important is that among others valleys 1 and 4 are depopulated, which causes the measured piezoresistance effects.

Interesting data concerning the relaxation time have been gained from Hall mobility measurements with stress in $[\bar{1}12]$ direction. For the current flow the longitudinal as well as transverse configuration was selected. The resulting Hall mobility μ_H versus electron concentration N_{inv} is plotted in Fig. 8. For a compression of $P = 190$ N/mm² we can assume that the domain structure collapses and mainly the paramagnetic state with valleys 1 and 4 exists. Tension depopulates these two valleys and the remaining four valleys still combine to a domain structure. This statement will be verified below by anisotropic conductivity data.

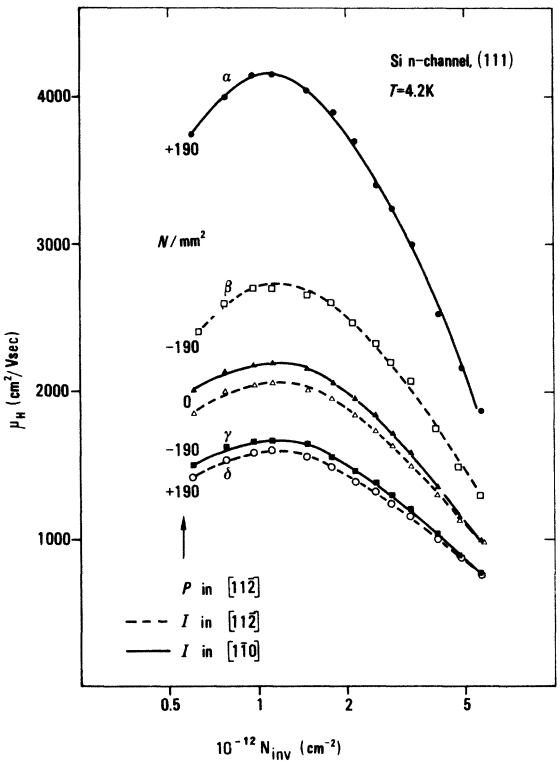

FIG. 8. Stress-dependent Hall mobility μ_H as a function of electron concentration N_{inv} for a (111) surface orientation at 4.2 K (magnetic field $B = 1$ T). The dashed profiles correspond to a current I in $[11\bar{2}]$ direction; the full lines to a current I in $[1\bar{1}0]$ direction. △,▲, without stress; ○,●, compression; □,■, tension.

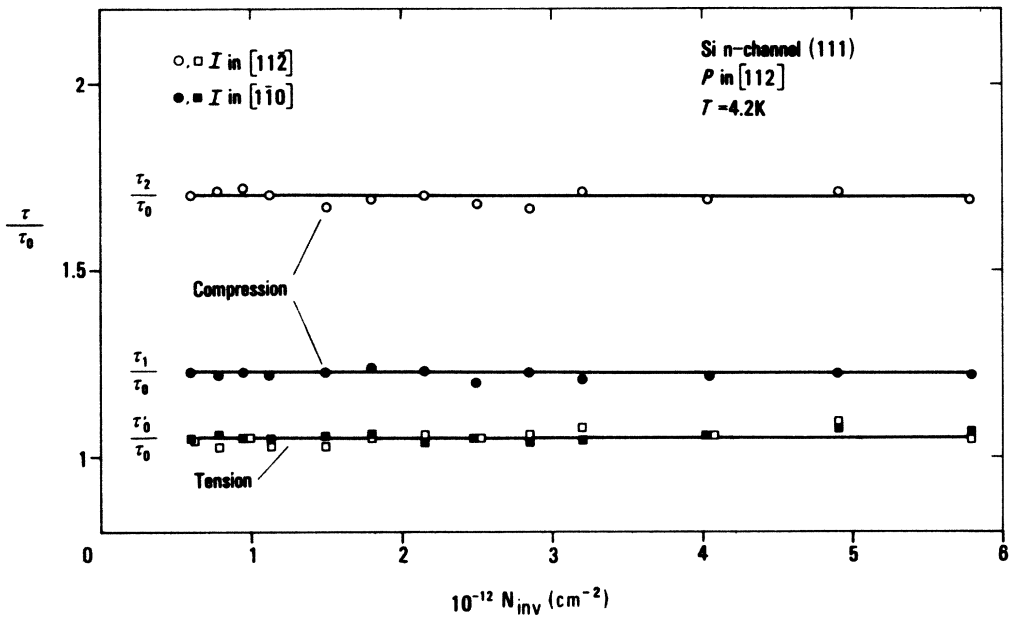

FIG. 9. Normalized relaxation times vs electron concentration N_{inv} for a (111) surface at 4.2 K. Parameter is the mechanical stress P.

To eliminate effects due to differences in transistor quality the mobility ratio between the stressed and unstressed sample is evaluated. In order to gain information about relaxation times, the mobilities are normalized with respect to the effective-transport masses according to

$$\begin{aligned}
&\frac{\tau_2}{\tau_0}=\frac{\mu_\delta}{\mu_0}\frac{2m_T+m_L}{3m_T} \text{ for } I \text{ in } [11\bar{2}]\,,\\
&\frac{\tau_1}{\tau_0}=\frac{\mu_\alpha}{\mu_0}\frac{2m_T+m_L}{m_T+2m_L} \text{ for } I \text{ in } [\bar{1}10]\,,\\
&\frac{\tau_0'}{\tau_0}=\frac{\mu_\beta}{\mu_0}\frac{2(2m_T+m_L)}{3(m_T+m_L)} \text{ for } I \text{ in } [11\bar{2}]\,,\\
&\frac{\tau_0'}{\tau_0}=\frac{\mu_\gamma}{\mu_0}\frac{4m_T+2m_L}{m_T+m_L} \text{ for } I \text{ in } [\bar{1}10]\,,
\end{aligned} \tag{14}$$

where m_T and m_L are the transverse and longitudinal bulk masses of silicon, respectively. The reference relaxation times for the two unstressed transistors are labeled with τ_0. τ_0' corresponds to the relaxation time under tension. τ_1 and τ_2 characterize the relaxation times under compression. For the paramagnetic states they correspond to the values along the small and large semiaxis of the subband ellipses, respectively. The evaluation of Fig. 8 with help of Eq. (14) is presented in Fig. 9. Apparently tension has no significant influence on the relaxation time, i.e., the domain structure is retained. Compression increases τ remarkably which is interpreted as the achievement of the paramagnetic state and a diminishing domain wall scattering. The difference between τ_1 and τ_2 can be ascribed to the anisotropy of the relaxation time of the elliptical constant-energy surfaces. $\tau_2 = 1.38\tau_1$ agrees surprisingly well with data obtained for the (110) surface.[18] The profiles are independent of electron concentration, which favors the idea that only the magnitude of the mechanical stress and not the position of the Fermi level is responsible for the annihilation of the domain structure.

The increase of the relaxation time under compression can be used to estimate the influence of domain scattering. Assuming that the scattering mechanisms are independent of each other one can write

$$\frac{1}{\tau}=\sum_i \frac{1}{\tau_i}+\frac{1}{\tau_D}\,, \tag{15}$$

where τ_i represents the known scattering effects (Coulomb, roughness, lattice) and τ_D corresponds to domain wall scattering. Because $1/\tau_D$ is negligible for high compression the Hall mobility data can be used to determine τ_D for the unstressed case. In connection with the mean velocity of the electrons the mean free path related to domain scattering can be estimated. For a concentration $N_{inv} = 1\times 10^{12}$ cm^{-2} this value amounts to 250 nm and represents a crude measure for the domain size.

C. Anisotropic Conductivity

The anisotropic conductivity characterized by the electric field ratio E_y/E_x is shown in Fig. 10(a) for three surface orientations at 4.2 K. For the (100) surface, stress P is applied in [001] and the electric field E_x in [011] direction; for the (110) surface, P in [001] and E_x in $[1\bar{1}1]$; and for the (111), surface P in $[11\bar{2}]$ and E_x in $(1-\sqrt{3}, 1+\sqrt{3}, -2)$. At $P=0$ only the (110) surface has a pronounced anisotropy as is expected from the ground state population of valleys 1, 2, 3, 4. Electron-transfer effects under stress will be analyzed on the basis of Eq. (8) which is generally valid for many valley semiconductors. For our three particular surfaces this equation has been evaluated with respect to electron concentrations. The obtained relation can be simplified by considering the valley shift due to the applied stress. The normalized concentrations in specific valleys selected by the stress direction are finally given by

$$\text{(100)}: \frac{n_{3+5}}{N_{\text{inv}}} = \frac{2\mu_T E_y/E_x}{(\mu_T-\mu_L)(1+E_y/E_x)},$$

$$\text{(110)}: \frac{n_{5+6}}{N_{\text{inv}}} = \frac{\mu_T-\mu_L+(\mu_T+\mu_L)E_y/E_x}{2\mu_T-\mu_P-\mu_L+(\mu_L-\mu_P)E_y/E_x}, \quad (16)$$

$$\text{(111)}: \frac{n_{1+4}}{N_{\text{inv}}} = \frac{1}{3} - \frac{2}{3}\left(\frac{\mu_T+\mu_P}{\mu_T-\mu_P}\right)E_y/E_x,$$

where μ_P is the mobility related to the principal mass. for (110) $m_P=(m_T+m_L)/2$ and for (111) $m_P=(m_T+2m_L)/3$. Assuming a constant relaxation time, the normalized concentration[34] is evaluated versus stress in Fig. 10(b). It should be noted that the results are somewhat inaccurate because for anisotropic valleys, τ is also anisotropic. From $\tau_2=1.38\tau_1$ it can be estimated, however, that the concentration ratio increases by no more than 12%.

For all three surface orientations it is obvious that for low concentrations such as $N_{\text{inv}}=8\times10^{11}$ cm^{-2} a mechanical stress of approximately 200 N/mm^2 is big enough to cause almost a complete electron transfer into specific anisotropic valleys with a quantum-limit ground state. The transition between two limiting states is continuous, which means that in this region at least four valleys are populated. Therefore the probability of correlation effects is given for all three surface orientations. In connection with the fact that $g_v=2$ is inevitable under all conditions, Fig. 10(b) suggests the existence of a domain structure.

With stress as parameter the anisotropy E_y/E_x finally has been studied as a function of temperature. The results for the (111) surface with stress in $(1-\sqrt{3}, 1+\sqrt{3}, -2)$ and E_x in $[11\bar{2}]$ direction are presented in Fig. 11, and for the (100) surface with stress in [001] and I in [011] direction in Fig. 12. Around $T_c=280$ K for both orientations a stress-independent kink occurs which cannot be understood with the "classical" population effect. For comparison, the theoretical profile for $P=180$ N/mm^2 is shown in Fig. 11. Below the critical temperature T_c experiment and theory disagree by about a factor of 3.

The discrepancies can once more be explained by intervalley coupling. The additional effect could arise from the stress-induced energy separation which lifts valleys 2 and 5 so far that coupling effects with them become unlikely. This in turn causes an increase of the electron concentration in domains containing valleys 3 or 6. Because 3 as well as 6 determine E_y/E_x, the total anisotropy effect increases. The (100) results can be interpreted in a similar manner. Below T_c the anisotropy effect E_y/E_x is enhanced with a slightly stress dependent maximum around 80 K.

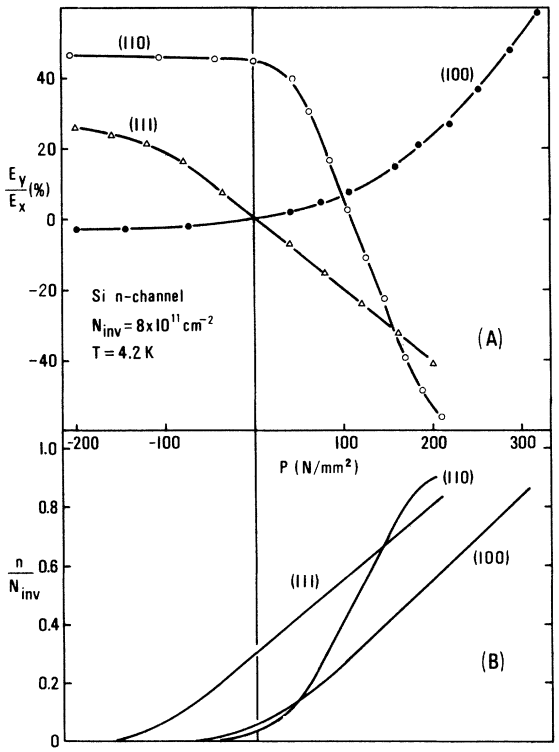

FIG. 10. (a) Anisotropic conductivity E_y/E_x plotted against mechanical stress P for (100), (110), and (111) surface orientations. The electron concentration $N_{\text{inv}}=8\times10^{11}$ cm^{-2} corresponds to all three orientations. The temperature was 4.2 K. (b) Corresponding population effects normalized with respect to total electron concentration N_{inv}.

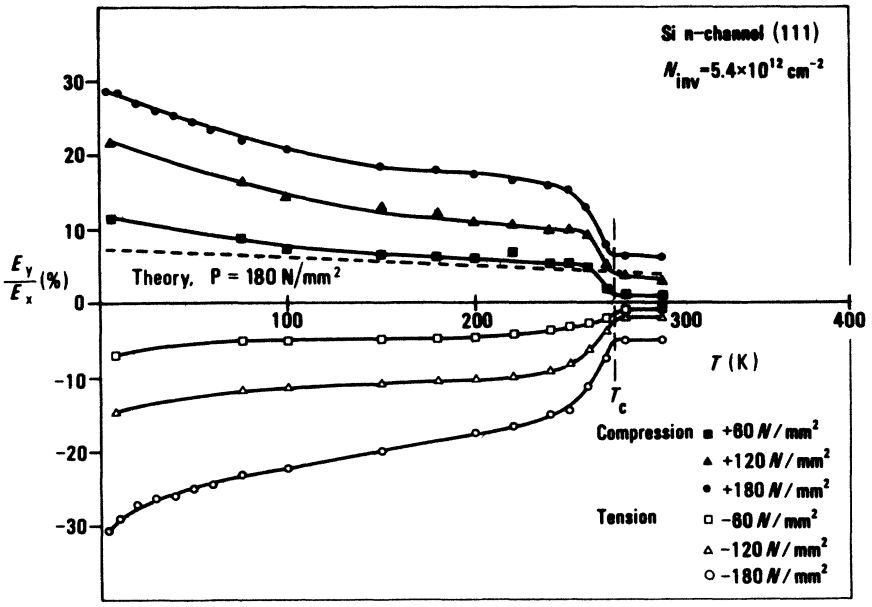

FIG. 11. Temperature dependence of the anisotropic conductivity E_y/E_x for a (111) surface. Parameter is the mechanical stress P in $(1-\sqrt{3}, 1+\sqrt{3}, -2)$ direction. Current is applied in $[11\bar{2}]$ direction. The dashed line represents the theory without correlation effects. At $T_c = 280$ K a sharp kink in the profile occurs.

The decrease at low temperatures indicates that the decreasing thermal broadening lessens the population of anisotropic valleys, i.e., lessens the exchange interactions. This description agrees with the observed increase of the cyclotron mass with increasing temperature.[7] The mass change from $0.2m_0$ to $0.3m_0$ which was only observed at low-electron concentrations, corresponds to the increased intervalley correlation between valleys 1-2 and 3-4-5-6. The fact that T_c is identical for both orientations hints that not the shape of the Fermi surfaces but the phonon spectrum in silicon is important for the coupling.

V. CONCLUSION

For the investigated surface orientations a valley degeneracy $g_v = 2$ was measured independent

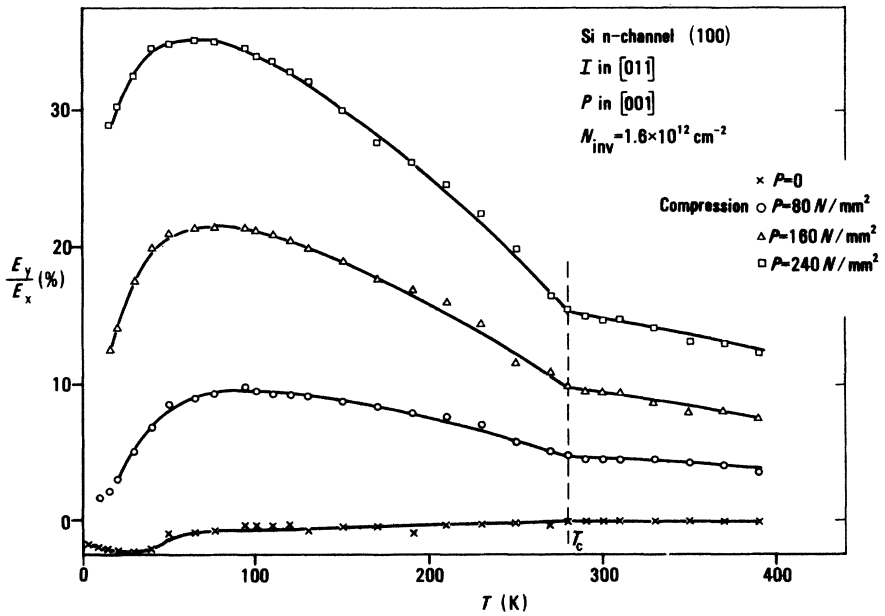

FIG. 12. Temperature dependence of the anisotropic conductivity E_y/E_x for a (100) surface. Parameter is the mechanical stress in [001] direction. Current I is applied in [011] direction. At $T_c = 280$ K a kink in the profile occurs.

of electron concentration and applied stress up to $P = 320$ N/mm^2. In connection with a completely isotropic conductivity for the (111) surface a domain model has been postulated which is based on intervalley interactions. They can be described by the existence of CDW due to a phonon-assisted interaction between electrons in different valleys. As a result a favorable ground state occurs which is energetically lowered by the interaction.[9] The experiments presented in this paper indicate that the described new ground state is dominant whenever the quantized subband levels of different valleys are populated and approach an equal level. The coupling influences the effective masses and the mean free path of the electrons in the inversion layer.

Pronounced cyclotron mass changes have been found for the (100) and (110) surfaces where the coupling takes place between subbands with different constant energy surfaces. The data are in agreement with cyclotron resonance experiments[6] exhibiting only one resonance peak which under stress shifts from $m_c = 0.2m_0$ to $m_c = 0.4m_0$. Remarkable temperature-dependent effective masses measured with cyclotron mass experiments[7] can also be well understood on this basis if a temperature-dependent overlap of the subbands is assumed.

The creation of domains decreases the mean-free path of the electrons, i.e., the relaxation time. It can be interpreted as scattering on domain walls and explains successfully piezoresistance and Hall-effect measurements. An interesting result yields the analysis for the (111) surface, where the anisotropy of the relaxation time for the elliptical constant-energy surface has been determined to be $\tau_2 = 1.38\tau_1$.

The existence of domains based on intervalley coupling described by CDW is only expected below a critical temperature T_c. The temperature dependence of the stress-induced anisotropic conductivity hints that T_c could be near room temperature. This large value is surprising but comparable data have been measured for layered compounds.[35] An interesting question which has not been solved up to now is the domain size. A crude estimate obtained from relaxation time measurements yields values between 200 and 300 nm. This size seems to be large enough to find an experimental way to directly visualize the existence of domains.

In conclusion we would like to point out that by assuming correlation effects which can be described by charge-density waves at the Si-SiO_2 interface a consistent explanation of all the presented experimental data can be achieved. This is an important result and has to be considered for further investigations of inversion layers in semiconductors.

ACKNOWLEDGMENTS

The authors are indebted to E. F. Krimmel and P. J. Stiles for valuable discussions. We also would like to thank E. Doering for the device fabrication and R. Schreiter and Z. Cehovec for technical assistance.

[1]For a review, see G. Dorda, in *Festkörperprobleme XIII* (Pergamon-Vieweg, Braunschweig, 1973), p. 215.
[2]T. Neugebauer, K. von Klitzing, G. Landwehr, and G. Dorda, Solid State Commun. 17, 295 (1975).
[3]A. Lakhani and P. J. Stiles, Phys. Lett. 51A, 117 (1975).
[4]G. Dorda, H. Gesch, and I. Eisele, Solid State Commun. 20, 429 (1976).
[5]I. Eisele, H. Gesch, and G. Dorda, Surf. Sci. 58, 169 (1976).
[6]P. Stallhofer, J. P. Kotthaus, and J. F. Koch, Solid State Commun. 20, 519 (1976).
[7]H. Kühlbeck and J. P. Kotthaus, Phys. Rev. Lett. 35, 1019 (1975).
[8]D. C. Tsui and G. Kaminsky, Solid State Commun. 20, 93 (1976).
[9]M. J. Kelly and L. M. Falicov, Phys. Rev. Lett. 37, 1021 (1976); Phys. Rev. B 15, 1974 (1977).
[10]M. J. Kelly and L. M. Falicov, Solid State Commun. 22, 447 (1977).
[11]S. Kawaji, J. Phys. Soc. Jpn. 27, 906 (1969).
[12]C. T. Sah, T. H. Ning, and L. L. Tschopp, Surf. Sci. 32, 561 (1972).
[13]H. Ezawa, Ann. Phys. (N.Y.) 67, 438 (1971).
[14]H. Ezawa, Surf. Sci. 58, 25 (1976).
[15]F. Stern and W. E. Howard, Phys. Rev. 163, 816 (1967).
[16]G. Dorda and I. Eisele, Phys. Status Solidi A 20, 263 (1973).
[17]S. J. Fonash, J. Appl. Phys. 44, 4607 (1973).
[18]H. Sakaki and T. Sugano, in Proceedings of the Third Conference on Solid State Devices, Tokyo, 1971 (unpublished); Oyo Buturi Suppl. 41, 141 (1972).
[19]G. Landwehr, *Festkörperproblem XV* (Pergamon-Vieweg, Braunschweig, 1975), p. 49.
[20]L. M. Roth and P. N. Argyres, in *Semiconductors and Semimetals* (Academic, New York, 1966), Vol. 1, p. 159.
[21]E. Bangert (private communication).
[22]T. Ando, J. Phys. Soc. Jpn. 37, 1233 (1974).
[23]J. R. Brews, J. Appl. Phys. 46, 2193 (1975).
[24]E. P. Jacobs and G. Dorda, Surf. Sci. (to be published).
[25]I. Eisele and G. Dorda, Solid State Commun. 15, 1391 (1974).
[26]W. Paul and D. M. Warschauer, in *Solid Under Pressure* (McGraw-Hill, New York, 1963), p. 245.
[27]I. Eisele, H. Gesch, and G. Dorda, Solid State Commun. 20, 677 (1976).
[28]J. L. Smith and P. J. Stiles, Phys. Rev. Lett. 29, 102 (1972).

[29]F. Stern, Phys. Rev. B 5, 4891 (1972).
[30]T. Ando, Phys. Rev. B 13, 3468 (1976).
[31]F. Stern (private communication).
[32]F. F. Fang and A. B. Fowler, Phys. Rev. 169, 619 (1968).
[33]G. Dorda, I. Eisele, E. Soutschek, K. Hess, in Proceedings of the Third International Conference on Solid Surfaces, Vienna, 1977 (unpublished).
[34]For the (100) surface at low concentrations, E_y/E_x become <0 because under tension a small-electron concentration remains in valleys 4 and 6 due to inhomogeneities. This has been included for the calculation of n_{3+5}.
[35]F. J. DiSalvo, Surf. Sci. 58, 297 (1976).